의학박사 학위논문

후각 소실에서 비강 내 니코틴아미드 아데닌 디뉴클레오타이드 투여의 치료 효과 연구

Therapeutic effect of intranasal nicotinamide adenine dinucleotide in restoration of olfactory dysfunction

울 산 대 학 교 대 학 원

의 학 과

유 신 혁

Therapeutic effect of intranasal nicotinamide adenine dinucleotide in restoration of olfactory dysfunction

지 도 교 수 김 지 희

이 논문을 의학박사학위 논문으로 제출함

2024년 8월

울 산 대 학 교 대 학 원

의 학 과

유 신 혁

유신혁의 의학박사학위 논문을 인준함

심사위원 장 용 주 인

심사위원 정 유 삼 인

심사위원 모 지 훈 인

심사위원 김 지 희 인

심사위원 이 주 영 인

울 산 대 학 교 대 학 원

2024년 8월

Abstract

Olfactory dysfunction is a debilitating condition with no established treatment. This study aimed to assess the efficacy of intranasal (i.n.) administration of nicotinamide adenine dinucleotide (NAD) in restoring olfactory function.

Cultured human olfactory stem cells (hOSCs) were used to evaluate the therapeutic efficacy of NAD in vitro. Immunofluorescence (IF) staining, PCR, and Western blot analyses were employed to determine whether NAD treatment facilitated the differentiation of cultured hOSCs into olfactory sensory neurons (OSNs).

Four experimental groups were used for the in vivo study: control, NAD i.n. (NAD group), intraperitoneal (i.p.) injection of dexamethasone (DXM group), and anosmia (n = 10 per group). Chronic $ZnSO_4$ i.n. administration induced olfactory dysfunction in the mouse model. Intranasal administration of 20 μL $ZnSO_4$ (170 μM) in each nostril (40 μL in total) was performed three times a week for four weeks. The NAD group received daily NAD i.n, while the DXM group received DXM (1 mg/kg) i.p. injections once a week for four weeks. The control and anosmia groups mice were treated with daily i.n. phosphate-buffered saline (20 μL in each nostril; 40 μL in total). Restoration of olfactory function was evaluated using histological analysis and behavioral tests. Further investigation of the mechanism was performed via comprehensive gene expression analyses using RNA sequencing (RNA-seq).

IF staining of OSN markers (OMP, acetylated β-III tubulin) and neuronal stem cell markers (SOX2, nestin) revealed that NAD promoted the differentiation of hOSCs into OSNs in vitro. PCR analyses showed that NAD enhanced the expression of neuronal differentiation-related markers (*SOX2, NESTIN, NEUROD1, NEUROG1*, and *OMP*). Additionally, Western blot analysis demonstrated increased levels of SOX2, nestin, and OMP protein levels after NAD treatment.

In vivo, the olfactory function of the NAD group significantly improved by day 28 compared with the anosmia group, whereas the DXM group showed no improvement. Histological analyses revealed that the olfactory epithelium (OE) in the NAD group was

markedly repaired, with both the thickness of the OE and the number of OSNs significantly higher than those in the DXM and anosmia groups. Bulk RNA-seq of the olfactory turbinate tissue identified two unique gene expression patterns and 201 differentially expressed genes (DEGs). Of these, 113 DEGs (cluster T1) were upregulated in control and NAD group mice, while 88 DEGs (cluster T2) were downregulated exclusively in control mice. Gene ontology terms associated with Cluster T1 included "modulation of chemical synaptic transmission", "regulation of nervous system process", and "response to steroid hormone". Cellular deconvolution using a validated public single-cell RNA sequencing (scRNA-seq) dataset identified candidate genes expressed in olfactory receptor neurons. Twenty-five genes implicated in the modulation of synaptic chemical transmission were upregulated after NAD stimulation. Six candidate genes were identified by intersecting them with neuronal marker genes acquired from scRNA-seq analysis data: *ABHD2, DLGAP2, FOXO3, HIPK2, KCNMA1,* and *PCDH17*. These genes were significantly upregulated in the NAD group compared with the anosmia group, with their expression levels restored to those observed in the control group. PCR analysis confirmed significantly higher expression levels of DLGAP2, FOXO3, HIPK2, and PCDH17 in differentiated hOSCs treated with NAD in vitro.

This study demonstrated the potential therapeutic efficacy of NAD for regenerating OSNs in vitro and restoring olfactory function in mice with anosmia. Our comprehensive evaluation indicated promising outcomes for the use of NAD as a potential treatment for olfactory dysfunction.

Keywords: olfaction, anosmia, intranasal administration, nicotinamide adenine dinucleotide

Table of Contents

Lists of Figures

Lists of Tables

INTRODUCTION

Olfactory dysfunction, estimated to affect 3–20% of the worldwide population, substantially impacts individual well-being and quality of life, and can increase mortality risk by up to four times.(1-4) This increased risk is primarily due to the compromised ability of the immune system to detect potentially harmful signals such as fires, toxic chemical fumes, gas leaks, and rotting food.(5-7) The treatment approach for olfactory dysfunction depends on its underlying cause and may include surgery, olfactory training, and oral or intranasal (i.n.) steroid sprays.(8-10) However, the management of this condition is challenging given the effectiveness of these treatments is not guaranteed.(11)

Nicotinamide adenine dinucleotide (NAD) is a coenzyme found in all living cells, existing in two forms: NAD^+ (oxidized) and NADH (reduced). Within the mitochondria, the ratio of NAD^+ to NADH is maintained at 7–8, whereas in the cytoplasm, it ranges from 1 to 700 under healthy conditions.(12) NAD is continuously produced, consumed, and recycled within cells, allowing for dynamic regulation. Mammals synthesize NAD through three primary pathways: the *de novo* pathway using tryptophan, the Press–Handler pathway using nicotinic acid, and the salvage pathway using nicotinamide.(13) Enzymes that consume NAD include sirtuins, sterile alpha and Toll/interleukin-1 receptor motif-containing 1 (SARM1), cluster of differentiation 38 (CD38), and poly ADP–ribose polymerases (PARPs).(14, 15) Beyond its role in redox reactions,(16) NAD is crucial for various physiological processes such as energy metabolism, transcriptional regulation, and DNA repair.(17-19) It also influences pathological processes linked to inflammation, cancer, and neurodegeneration.(20) Recent research indicates that NAD deficiency is associated with inflammation, poor DNA repair, and mitochondrial dysfunction, whereas increased NAD levels enhance metabolic fitness.(21) Additionally, NAD is vital for energy metabolism and mitochondrial activities, including calcium homeostasis, gene expression, aging, and cell death.(12) Numerous studies have demonstrated the therapeutic potential of NAD in neurological disorders.(22, 23) Given these insights, NAD may have the potential to manage olfactory dysfunction caused by injury

to the olfactory sensory neurons (OSN) of the olfactory epithelium (OE), although no studies have specifically explored this application.

In this study, we cultured and treated human olfactory stem cells (hOSCs) with NAD to determine whether NAD facilitates their differentiation into OSNs. We also aimed to investigate whether i.n. delivery of NAD could enhance the restoration of olfactory dysfunction in a mouse model of olfactory impairment. Behavioral tests and histological analyses were performed to assess the restoration of olfactory function and regeneration of the OE. Further mechanistic insights were obtained through RNA sequencing (RNA-seq).

MATERIALS AND METHODS

Collection of olfactory mucosae in humans

The collection of human olfactory mucosa and isolation of hOSCs from tissues was performed following the protocol described by Girard *et al*.(24) Both nasal cavities were examined using a 0° or 30° rigid endoscope (4 mm diameter) to identify polyps or inflammatory lesions. The optimal nasal cavity was chosen based on septal deviation. Lidocaine with epinephrine was applied as a local anesthetic for 10 minutes using a cotton applicator. Biopsy was performed using ethmoid forceps to obtain a 2 mm^2 tissue sample from either the root of the medial aspect of the middle turbinate or the dorsomedial area of the septum. The tissue was transferred to a sterile 2 mL tube filled with 1 mL Dulbecco's Modified Eagle Medium supplemented with Ham's F-12 nutrient mixture (DMEM/HAM F12 [Gibco, Thermo Fisher Scientific, Waltham, MA, USA]) using a sterile needle. This study was conducted in accordance with the Declaration of Helsinki and was approved by the Institutional Review Board of Dankook University Hospital (IRB No. 2024-05-014).

Isolation of OSCs from human

Nasal mucosal tissues were washed in DMEM/HAM F12, followed by a 1-h incubation in dispase II solution (STEMCELL Technologies, Vancouver, Canada) (2.4 IU/mL) at 37°C. The OE was dissected from the underlying lamina propria using a microspatula under a dissecting microscope (Olympus, Tokyo, Japan). Differential characteristics such as the translucent appearance of the epithelium against a black background and striped orange/brown lamina propria were noted. The lamina propria was then transferred to a Petri dish containing DMEM/HAM F12 and sliced into pieces (200–500 μm thickness). These pieces were placed in 2 cm diameter culture dishes, covered with sterile glass coverslips, and supplemented with 500 μL of culture medium (DMEM/HAM F12 supplemented with 10% fetal bovine serum [FBS] and antibiotics). The medium was renewed every 2–3 d. Stem cell invasion began within

5–7 d, and confluency was achieved after two weeks. Cells were passaged and transferred to culture flasks.

Cell viability assay of NAD for hOSCs

hOSCs within five passages were seeded at 1×10^6 cells/mL in a 96-well plate containing 50 μL/well of DMEM/F12 with 10% FBS. Cells were treated with NAD stock solution (50 mM in DMEM/F12 within 10% FBS) at final concentrations of 0–20 mM. After 24 h of culture in a CO_2 incubator, 10 μL/well of CCK-8 reagent (DOJINDO Laboratories, Kumamoto, Japan) was added. After a 2-h incubation, optical density (OD) was measured at 450 nm using a microplate reader (Thermo Fisher Scientific, Waltham, MA, USA). The OD of cells at 0 mM NAD was considered 100% cell viability, and the relative viability of cells treated with other NAD concentrations was calculated.

Neuronal differentiation of hOSCs

Neuronal differentiation of hOSCs was induced using Neurobasal medium and DMEM/F12 medium supplemented with B-27, L-glutamine (GlutaMAX, Gibco, Thermo Fisher Scientific), glutamate (2 mM), penicillin (50 U/mL), and streptomycin (50 μg/mL). To evaluate the effect of NAD on neuronal differentiation, hOSCs were incubated with Neurobasal medium containing 2.5 or 5.0 mM NAD, with the medium changed every 3 d.

PCR analyses

Quantitative real-time PCR was performed using the RIboEx^{TM} reagent (GeneAll Hybrid R kit, GeneAll Biotechnology Co., Ltd., Seoul, Republic of Korea) to extract total RNA from hOSCs treated with NAD, following the manufacturer's instructions. RNA was reverse transcribed using an iScript cDNA Synthesis Kit (Gene All Biotechnology Co., Ltd.). mRNA expression was analyzed using an Applied Biosystems 7500 Real-Time PCR System (Applied Biosystems, Waltham, MA, USA). The relative mRNA expression levels of *DLGAP2,*

FOXO3, HIPK2, PCDH17, SOX2, NESTIN, NEUROG1, NEUROD1, OMP, and *GAPDH* were evaluated using SYBR Green primers from Bioneer (Daejeon, Republic of Korea) and Applied Biosystems (Table 1). Relative mRNA expression was calculated using the 2-ΔΔCt method and normalized to *GAPDH*.

Table 1. Primers used in PCR analysis to determine the extent of differentiation of hOSCs treated with NAD

Genes	Forward (5′-3′)	Reverse (5′-3′)
DLGAP2	CCTCTGACATCACCTCCACCAT	TCACCGAGATCAGAGGCTTGGA
FOXO3	TCTACGAGTGGATGGTGCGTTG	CTCTTGCCAGTTCCCTCATTCTG
HIPK2	AGCGTCATCACCATCAGCAGTG	AGTCGTGGACTGTGACACAGCT
PCDH17	CAAAGGCTCCTGCTGTGACATG	GACCAAGCACTCGGCATTCATC
SOX2	GCTACAGCATGATGCAGGACCA	TCTGCGAGCTGGTCATGGAGTT
NESTIN	TCAAGATGTCCCTCAGCCTGGA	AAGCTGAGGGAAGTCTTGGAGC
NEUROD1	GGTGCCTTGCTATTCTAAGACGC	GCAAAGCGTCTGAACGAAGGAG
NEUROG1	GCCTCCGAAGACTTCACCTACC	GGAAAGTAACAGTGTCTACAAAGG
OMP	CAAGGAGGACTCGGATGCCATA	TCGCCAAAGGTGACGAGGAAGT
GAPDH	AGGTCGGTGTGAACGGATTT	TGTAGACCATGTAGTTGAGG

Western blot analyses

Total cell lysates (20–50 μg per well) were subjected to 10–12% SDS-PAGE and electrotransferred to nitrocellulose membranes (Amersham™ Protran, Cytiva, Malborough, MA, USA). Membranes were then incubated with primary antibodies against SOX2 (1:1000), nestin (1:1000), OMP (1:1000, Santa Cruz Biotechnology, Dallas, TX, USA), and β-actin (1:5000, Sigma-Aldrich, St. Louis, MO, USA), followed by secondary antibodies (horseradish peroxidase anti-rabbit or anti-mouse). Protein bands were detected using ECL Western blotting

substrate (Pierce™ ECL Western Blotting Substrate, Thermo Fisher Scientific) and imaged with the Gel Doc image analysis system (Bio-Rad, Hercules, CA, USA).

Anosmia mouse model

Forty female BALB/c mice (6–7 weeks old, 18–20 g; Orient Bio Inc., Sungnam, Republic of Korea) were divided into four groups (n = 10 per group): control, $ZnSO_4$-induced anosmia group, NAD i.n. treatment, and dexamethasone (DXM) intraperitoneal (i.p.) injection (Figure 1A and 1B).

Anosmia was induced by administering 20 μL $ZnSO_4$ (170 μM) i.n. in each nostril (total 40 μL), three times a week for a total of four weeks. Control mice received i.n. phosphate-buffered saline (PBS). Mice were housed in a specific pathogen-free biohazard containment facility. All experiments adhered to the National Institutes of Health Guide for the Care and Use of Laboratory Animals and were approved by the Institutional Animal Care and Use Committee of the Asan Institute for Life Sciences (2019-02-165).

Intranasal NAD administration

The NAD group received 100 mg/kg/day NAD (Sigma-Aldrich) i.n. daily for four weeks from Monday to Friday, starting one week after anosmia induction, administered in the head-down position. Control and anosmia groups received i.n. PBS, while the DXM group received 1 mg/kg i.p. DXM once a week for four weeks.

Behavioral tests and tissue preparation

Food-finding behavioral tests were conducted weekly to assess olfactory function (Figure 1A and 1B). Induction and recovery from anosmia were assessed using a food-finding test. Mice were food-deprived for one day, then released into an open field (buried food test) and T-maze (T-maze test) for 3 min each to find buried food pellets. The food pellets were buried randomly under the sawdust on one side of the cage (buried food test) or one arm of

the T-maze (T-maze test). Each test mouse started at the opposite corner of the pellet (buried food test) or at the base of the T (T-maze test) and then walked forward to find hidden food. The elapsed time to locate the food was recorded. Food-finding behavioral tests was performed at three times for each mouse. Mice were euthanized via cervical dislocation 24 h after the olfactory tests on day 28 for tissue sample collection and histological analysis.

Figure 1. Schematic illustration of in vivo experiment and behavioral test. (A) Behavioral tests (buried food and T-maze tests) of the $ZnSO_4$ anosmia mice model. (B) The anosmia mice model was generated by subjecting mice to weekly i.n. administration of $ZnSO_4$. The treatment group received daily i.n. administration of NAD, whereas the positive control group received weekly i.p. injection of dexamethasone (DXM). Behavioral tests were performed once every week for one month, and mice were euthanized for tissue analyses on day 28.

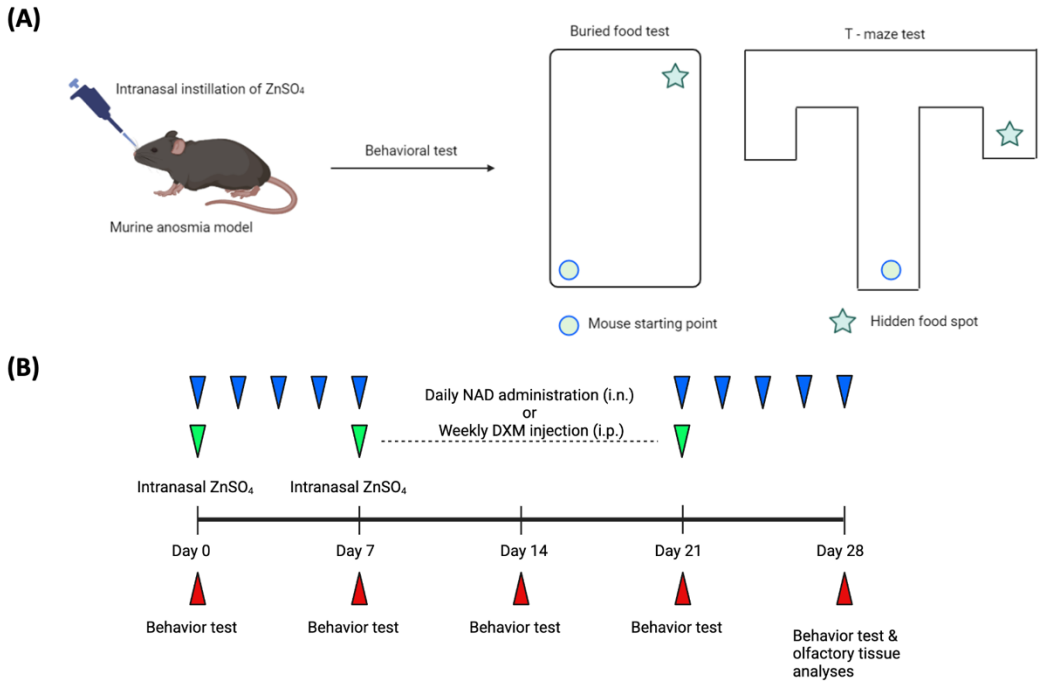

Hematoxylin and eosin (H&E) staining and tissue analysis

For histological analysis, mouse heads were collected after euthanasia, fixed in 10 % neutral buffered formalin, decalcified with 14 % ethylenediaminetetraacetic acid (EDTA) for three weeks, and embedded in paraffin. To evaluate the overall structure of nasal mucosa, 4-μm-thick paraffin sections were deparaffinized in xylene, rehydrated in alcohol, and stained with H&E (BBC Biochemical, Dallas, TX, USA). The nasal mucosal tissues were observed under a bright-field microscope (Olympus, Tokyo, Japan) at 200× magnification. The thickness of the OE on H&E-stained slides was measured to assess the degree of OE recovery in each mouse.

Immunofluorescent (IF) staining and tissue analysis using confocal microscopy

For in vitro confocal imaging, IF staining was performed to assess the stemness and differentiation of hOSCs after treatment with different concentrations of NAD. SOX2 and nestin staining were performed on hOSCs to evaluate their stemness following NAD treatment. Briefly, hOSCs were fixed with 4 % paraformaldehyde, washed with PBS, permeabilized with 0.5 % Triton X-100, and then blocked with 5 % bovine serum albumin (Sigma-Aldrich). Subsequently, cells were incubated with primary antibodies, anti-SOX2 (1:100; Abcam, Cambridge, UK) and anti-nestin (1:100; Abcam) overnight at 4 °C. Cells were then washed with PBS and incubated with Alexa Fluor 488 goat anti-mouse (1:500; Invitrogen, Thermo Fisher Scientific) or Alexa Fluor 594 goat anti-rabbit (1:500; Invitrogen, Thermo Fisher Scientific) secondary antibodies for 1 h at 25 °C. Cell nuclei were counterstained with 4′, 6-diamidino-2- phenylindole (DAPI; Sigma-Aldrich).

Olfactory marker protein (OMP) and acetylated β-III tubulin (Tuj1) staining were conducted to evaluate the degree of differentiation of hOSCs following NAD treatment. Cells were incubated with the respective primary antibodies: OMP for mature OSNs (1:100; Thermo Fisher Scientific), and Tuj1 for immature OSNs (1:500; BioLegend, San Diego, CA, USA) overnight at 4 °C. Cells were then incubated with Alexa Fluor 488 goat anti-mouse (1:1000;

Invitrogen, Thermo Fisher Scientific) or Alexa Fluor 594 goat anti-rabbit (1:500; Invitrogen, Thermo Fisher Scientific) secondary antibodies for 1 h at 25 °C. Cell nuclei were counterstained with DAPI. Cells were observed and imaged under a confocal microscope (FV-3000; Olympus). The signal intensity was measured using the ImageJ software (National Institutes of Health, Bethesda, MD, USA). The thresholding function in the ImageJ software was used to convert the confocal images into binary mask images. Using photographs from the control group, the minimum and maximum threshold values were adjusted to highlight the areas of interest. Subsequently, these parameters were uniformly applied to each sample. After setting the threshold parameters, the geometry of each cell was used to highlight the area of interest. The percentage area of each selected cell (% area) was measured using the Analyze menu.

For confocal imaging of the mouse models, IF staining was performed to evaluate the status of immature or mature OSNs. Nasal mucosa tissues were incubated with the respective primary antibodies: OMP for mature OSNs (1:200) or Tuj1 for immature OSNs (1:500) overnight at 4 °C. The tissues were then washed with PBS and incubated with Alexa Fluor 594 goat anti-rabbit (1:500) or Alexa Fluor 488 goat anti-mouse (1:500) secondary antibodies for 1 h at 25 °C. Cell nuclei were counterstained with DAPI. The nasal mucosal tissues were assessed under a confocal microscope. The signal intensity, number of OMP^+ cells, and mean fluorescence intensity (MFI) of Tuj1 in OE were measured using the ImageJ software.

Bulk RNA-seq analysis from murine olfactory turbinate and bulb tissues

To analyze the bulk RNA-seq data, the reads were mapped to the mm10 genome using STAR version 2.7.1a with default parameters.(25) Subsequently, the aligned reads were converted into tag directories using HOMER version 4.11.1.(26) Each file was quantified using the "analyzeRepeats" script in HOMER. Gene expression levels in each sample were normalized by calculating the transcripts per kilobase million (TPM). Differentially expressed

genes (DEGs) were identified via DESeq2 analysis based on raw read counts.(27) The "getDifferentialExpression" command in HOMER was applied with criteria for significance defined as an adjusted *P*-value of < 0.05, more than a two-fold difference in expression levels, and an average FPKM > 2.

Single-cell RNA-seq data analysis

This study employed publicly available datasets and databases, including single-cell RNA-seq datasets from Oliva *et al*.(28) and Tepe *et al*.(29) In addition, publicly available single-cell RNA-seq (scRNA-seq) data (accession numbers GSE184117 and GSE121891) were also analyzed.(28, 29) The obtained bulk RNA-seq dataset was integrated with public scRNA-seq data. To ensure compatibility and uniformity in tissue localization, an integrated analysis of olfactory mucosa biopsies of healthy donors from GSE184117 with that of the mouse olfactory turbinate tissue bulk RNA-seq dataset was performed.

For the analysis, only cells in which mitochondrial RNA accounted for less than 10 % of the total RNA content were included. The data were integrated and anchored using the top 10,000 highly variable features identified using the variance-stabilizing transformation method. Subsequently, uniform manifold approximation and projection (UMAP) analysis was conducted and a nearest neighbor graph was constructed using the 'FindNeighbors' function in R version 4.3.0 (The R Foundation for Statistical Computing, Vienna, Austria). The "FindClusters" function was employed to identify cell clusters with the resolution parameter set to 0.5. Differential expression analysis used the "FindMarkers" and "FindAllMarkers" functions. Principal component analysis and clustering were conducted using Seurat in R.

Statistical analysis

All statistical analyses were performed using the GraphPad Prism 10 software (GraphPad Software, San Diego, CA, USA). Results are expressed as the mean ± standard

error of the mean (SEM). An independent sample *t*-test and one-way ANOVA variance were used to compare the results between the groups. Statistical significance was set at $P < 0.05$.

RESULTS

NAD promoted the differentiation of hOSCs into OSNs in vitro

To investigate the role of NAD in the differentiation of hOSCs into OSNs, hOSCs were cultured with various concentrations of NAD. Cell viability assays (CCK-8) were performed to determine the optimal NAD concentration. Two sets of NAD concentrations were tested: 0, 10, 12.5, 15, 17.5, and 20 mM (Figure 2A), and 0, 1, 2, 5, and 10 mM (Figure 2B). No significant differences in cell viability were observed, but NAD concentrations between 2.5 and 5.0 mM increased hOSC viability the most. Therefore, 2.5 and 5.0 mM NAD were used for subsequent differentiation experiments.

Figure 2. Cell viability assay results using CCK-8, confirming the optimal NAD dose. Two sets of NAD concentrations were tested: (A) 0, 10, 12.5, 15, 17.5, and 20 mM; and (B) 0, 1, 2, 5, and 10 mM (n = 3 in each group).

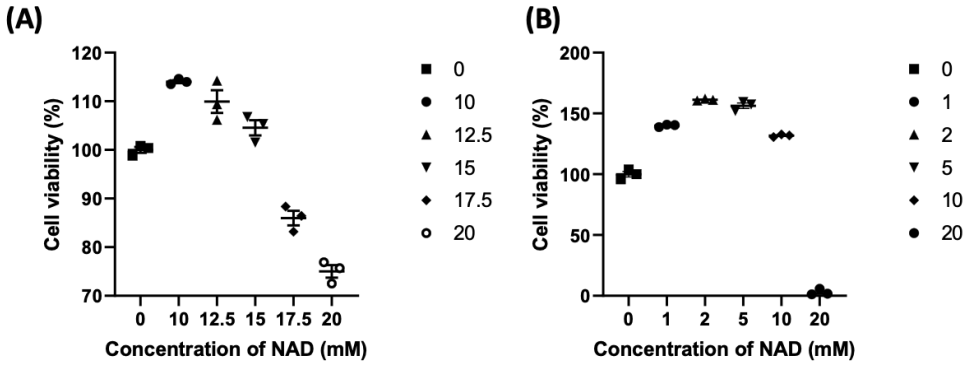

The potential of NAD administration to facilitate the differentiation of OSCs into OSNs was investigated through IF staining. To assess the extent of differentiation into immature or mature OSNs, IF staining was performed using Tuj1 and OMP antibodies one or two weeks after differentiation, with and without NAD administration (Figure 3A & 3B). At the end of the first week of differentiation, the mean $Tuj1^{+}$ intensity rate was 22.3 ± 6.2% in

the control group, 34.3 ± 18.9% in the 2.5 mM NAD group, and 65.5 ± 13.5 % in the 5.0 mM NAD group (Figure 3C). Statistically significant differences were observed when comparing the 2.5 mM and 5.0 mM NAD groups to the control group. By the second week, the mean $Tuj1^+$ intensity rate was 11.8 ± 5.3% in the control group, 60.8 ± 16.1% in the 2.5 mM NAD group, and 67.9 ± 12.1% in the 5.0 mM NAD group (Figure 3D). A significant increase in the Tuj1 signal, indicative of immature OSNs, was observed in the NAD-treated groups compared with the control group at the second week of differentiation.

Similar results were found for OMP, a marker of mature OSNs. After one week of differentiation, the mean OMP^+ intensity rate was 28.5 ± 3.6% in the control group, 41.7 ± 5.8% in the 2.5 mM NAD group, and 41.2 ± 2.3% in the 5.0 mM NAD group (Figure 3E). At the two-week mark, the mean OMP^+ intensity rate was 25.1 ± 4.7% in the control group, 51.4 ± 12.4% in the 2.5 mM NAD group, and 59.3 ± 7.5 % in the 5.0 mM NAD group (Figure 3F). The increases in OMP^+ intensity rates in the NAD treatment groups were statistically significant compared with the control group.

Figure 3. NAD promotes the differentiation of hOSCs into OSNs in vitro. Immunofluorescence staining distinguished immature OSNs (acetylated β-III tubulin [$Tuj1^+$] cells) from mature OSNs (olfactory marker protein, [OMP^+] cells) one (A) and two weeks (B) after neuronal differentiation with NAD administration (0, 2.5, and 5.0 mM). $Tuj1^+$ intensity was evaluated in the three groups (control, 2.5 mM NAD, and 5.0 mM NAD) at one (C) and two weeks (D) after differentiation. OMP^+ intensity was assessed at one (E) and two weeks (F). Statistical significance was determined using independent sample *t*-tests. * $P < 0.05$, ** $P < 0.01$, *** $P < 0.001$, n = 10 in each group.

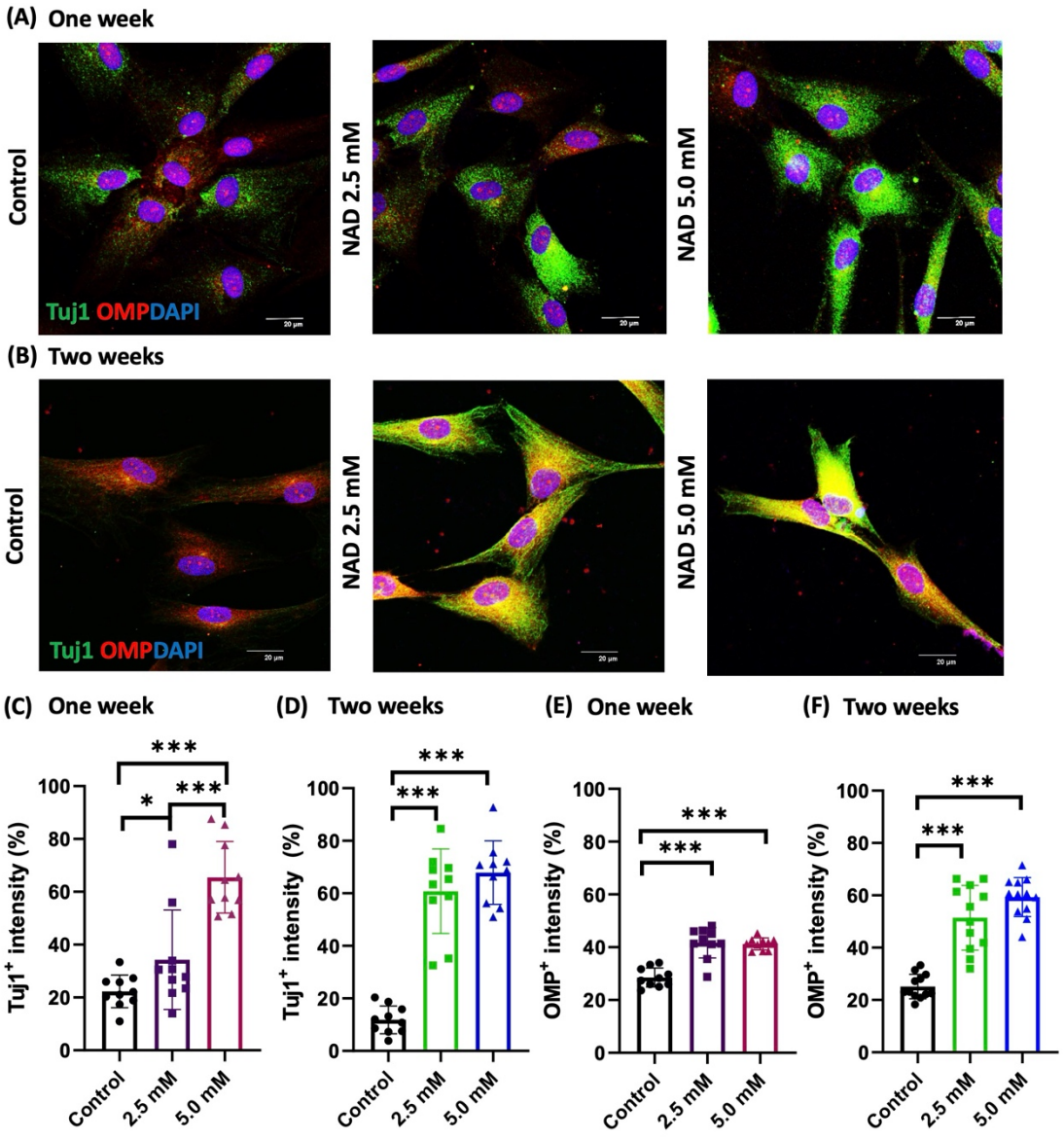

Additional IF staining was conducted to investigate the impact of NAD treatment on the expression of stem cell markers. SOX2 is widely recognized as a marker for multipotent neural stem cells.(30) SOX2 expression in OE is typically found in sustentacular cells and OSCs (horizontal and globose basal cells).(31) Nestin, another marker, is expressed in undifferentiated neural stem cells during development.(32) IF staining was performed using nestin and SOX2 antibodies one or two weeks after differentiation of hOSCs with or without NAD treatment (Figure 4A & 4B).

After the first week of differentiation, the mean nestin$^+$ intensity rate was 4.0 ± 1.7 % in the control group, 6.1 ± 1.4 % in the 2.5 mM NAD group, and 9.4 ± 1.5 % in the 5.0 mM NAD group (Figure 4C). Statistically significant increases in nestin$^+$ intensity were observed in the 2.5 mM and 5.0 mM NAD groups compared with the control group. In the second week, the mean nestin$^+$ intensity rate was 4.9 ± 1.8% in the control group, 6.6 ± 1.9% in the 2.5 mM NAD group, and 8.8 ± 2.7% in the 5.0 mM NAD group (Figure 4D). Notably, there was a statistically significant increase in nestin intensity in the 5.0 mM NAD group compared with the control group during the second week of differentiation.

Conversely, results for SOX2 staining showed a different pattern. At the first week of differentiation, the mean SOX2$^+$ intensity rate was 13.0 ± 3.7% in the control group, 33.1 ± 10.0% in the 2.5 mM NAD, and 54.4 ± 14.0% in the 5.0 mM NAD group (Figure 4E). Significant increases in SOX2 intensity were observed in the 2.5- and 5.0 mM NAD groups compared with the control group. By the second week, the mean SOX2$^+$ intensity rate was 3.2 ± 1.9% in the control group, 8.6 ± 3.0% in the 2.5 mM NAD, and 1.1 ± 1.3% in the 5.0 mM NAD group (Figure 4F). The SOX2$^+$ intensity was significantly higher in the 2.5 mM NAD group, whereas it was notably lower in the 5.0 mM NAD group compared with the control group.

Figure 4. Changes in immunofluorescence staining intensity of neural stem cell markers (nestin and SOX2) during hOSC neuronal differentiation with NAD treatment. Staining was performed at one (A, C, E) and two weeks (B, D, F) after differentiation with NAD administration (0, 2.5, and 5.0 mM). Nestin$^+$ intensity was evaluated in the control group, 2.5 mM NAD, and 5.0 mM NAD treatment groups at one (C) and two weeks (D) after neuronal differentiation. SOX2$^+$ intensity was also assessed at one (E) and two weeks (F) following neuronal differentiation. Statistical significance was determined using independent sample *t*-tests. * $P < 0.05$, ** $P < 0.01$, *** $P < 0.001$, n = 10 in each group.

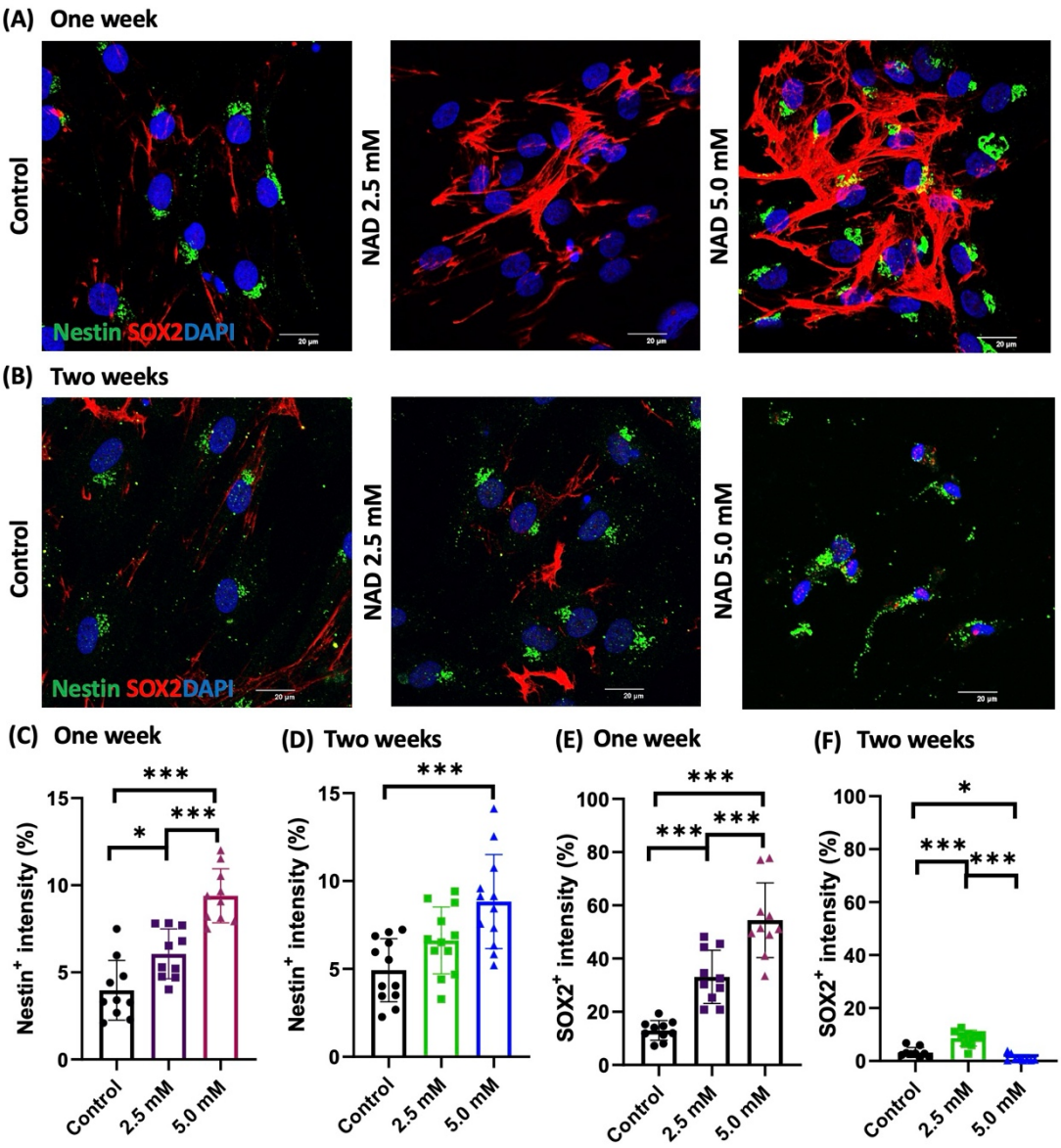

Additionally, PCR analyses were conducted to assess genes related to neuronal stem cells and immature and mature OSNs, including *SOX2* (Figure 5A), *NESTIN* (Figure 5B), *NEUROD1* (Figure 5C), *NEUROG1* (Figure 5D), and *OMP* (Figure 5E). The differentiated cell group showed significantly higher expression of all five genes compared with the undifferentiated OSC group. Specifically, *SOX2, NEUROD1, NEUROG1,* and *OMP* exhibited increased expression levels in the NAD treatment groups compared with the untreated group. Additionally, Western blot analysis was conducted to evaluate the expression levels of SOX2, nestin, and OMP associated with OSC and OSN (Figure 5F). The levels of SOX2, nestin, and OMP were higher in the NAD treatment groups compared with the untreated group.

Figure 5. Western blot and PCR analyses of marker genes and molecules associated with immature and mature OSNs and hOSCs. PCR analysis confirmed the expression of the following genes: *SOX2* (A), *NESTIN* (B), *NEUROD1* (C), *NEUROG1* (D), and *OMP* (E). (F) The expression of molecules associated with OSNs (OMP) and OSCs (SOX2 and nestin) was assessed using Western blot analysis. Experiments were conducted under four distinct conditions: differentiation (-), differentiation (+) without nicotinamide adenine dinucleotide (NAD), and differentiation (+) with 2.5 or 5.0 mM NAD. Statistical significance was determined using independent sample *t*-tests. * $P < 0.05$, ** $P < 0.01$, *** $P < 0.001$, n = 3 in each group.

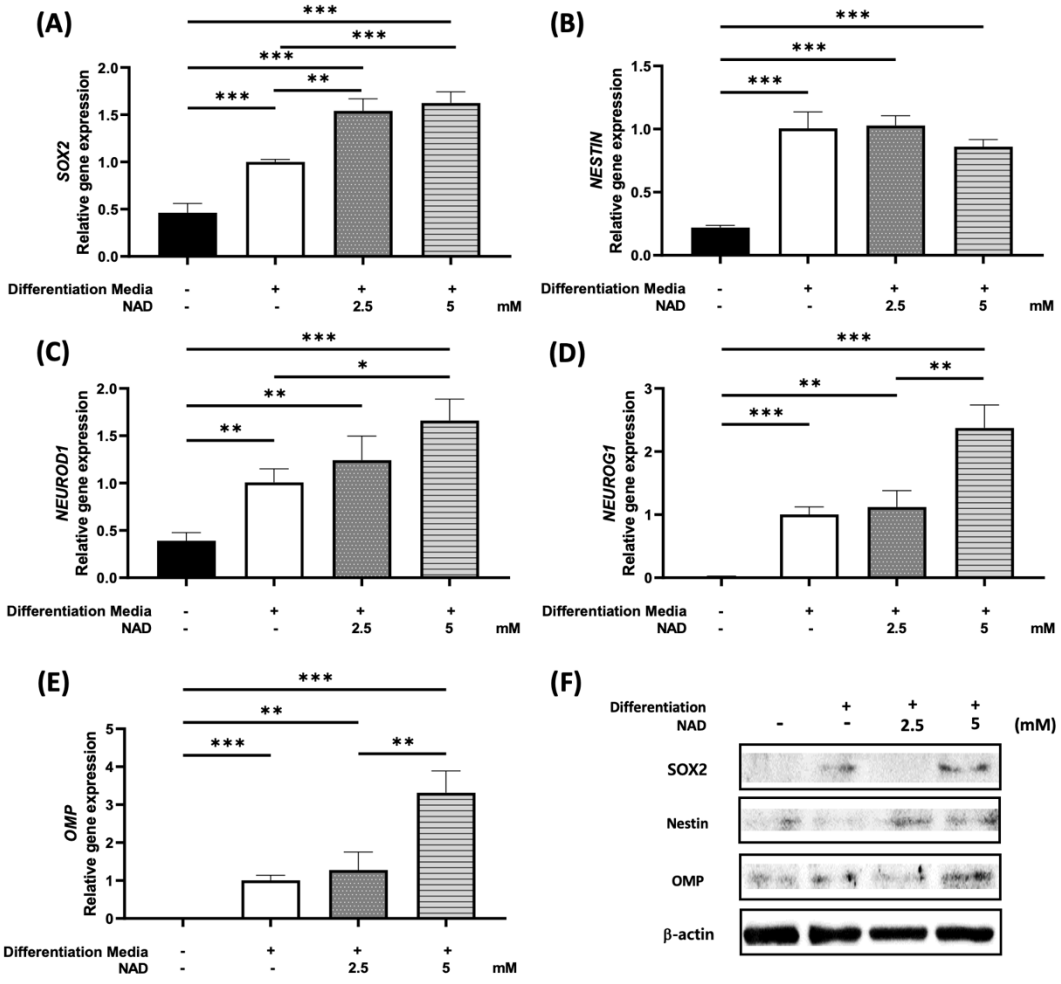

Intranasal administration of NAD improved olfactory function in anosmia mice

We used $ZnSO_4$ to create an anosmia mouse model. Briefly, NAD (i.n.) and DXM (i.p.) were administered to mice over four weeks. Behavioral tests were then conducted to evaluate the recovery of olfactory function in mice (Figure 1B).

Results from the open field and T-maze tests indicated that, compared with the DXM and anosmia groups, the olfactory function in the NAD group significantly improved by day 28 (Figure 6A and 6B). We noted that olfactory function steadily declined until day 14 across the anosmia, NAD, and DXM groups. However, improvement was observed in the NAD group by days 21 and 28 (Figures 6C and 6D).

These behavioral tests demonstrated that i.n. administration of NAD effectively restored olfactory function in the $ZnSO_4$-induced anosmia mouse model. Furthermore, NAD treatment outperformed DXM, the current conventional therapy for olfactory loss.

Histologic findings

After completing the olfactory behavioral tests on day 28, all mice were euthanized for histological analyses of their OE. The thickness of the OE layer was measured on hematoxylin and eosin (H&E)-stained slides (Figure 7A). Additionally, the total number of immature and mature OSNs was assessed using confocal microscopy (Figure 7B).

Mice in the control group exhibited the thickest mean OE layer, measuring 61.6 ± 5.8 μm. In contrast, the anosmia group had the thinnest mean OE layer at 15.2 ± 2.8 μm. The OE thickness in the DXM group varied widely, from 15.2 μm to 55.7 μm, with a mean of 31.0 ± 13.5 μm, significantly greater than the anosmia group ($P < 0.001$) but considerably lower than the control group ($P < 0.001$). The NAD group had a mean OE thickness of 52.9 ± 6.5 μm, significantly greater than the DXM and anosmia groups ($P < 0.001$) but significantly less than that the control group ($P < 0.01$) (Figure 7C).

The number of immature and mature OSNs in each OE group was evaluated using IF staining. The number of mature OSNs was determined using OMP staining (Figure 7D). The number of OMP^+ cells followed a trend similar to OE thickness. The control group had the highest mean number of OMP^+ cells per high power field (HPF) at 162.4 ± 15.0, while the anosmia group had the lowest mean number at 51.4 ± 20.4 cells/HPF. The DXM group had a mean OMP^+ cell of 63.8 ± 18.7 cells/HPF, which did not differ significantly from the anosmia group; in contrast, the NAD group had a mean OMP^+ cell count of 98.8 ± 24.6 cells/HPF, which was significantly higher than the anosmia group ($P < 0.001$).

Additionally, the number of immature OSNs in each group was evaluated using Tuj1 IF staining (Figure 7E). The Tuj1 mean MFI in the control group was 17.7 ± 8.2, which did not differ significantly from the DXM (15.4 ± 10.9) and anosmia groups (17.6 ± 16.6). However, the Tuj1 mean MFI in the NAD group was 43.1 ± 11.8, significantly higher than in the other three groups, indicating an increase in immature OSNs during the recovery phase following injury.

Figure 6. Intranasal administration of nicotinamide adenine dinucleotide (NAD) improved olfactory function in mice with anosmia. (A) Results of the buried food and (B) T-maze tests on day 28. (C) Results of the buried food test on days 0, 7, 14, 21, and 28. (D) Results of the T-maze test on days 0, 7, 14, 21, and 28. DXM, dexamethasone; i.n., intranasal administration; i.p., intraperitoneal injection. *P*-values were calculated using an independent sample *t*-test. * $P < 0.05$, ** $P < 0.01$, *** $P < 0.001$, n = 10 in each group.

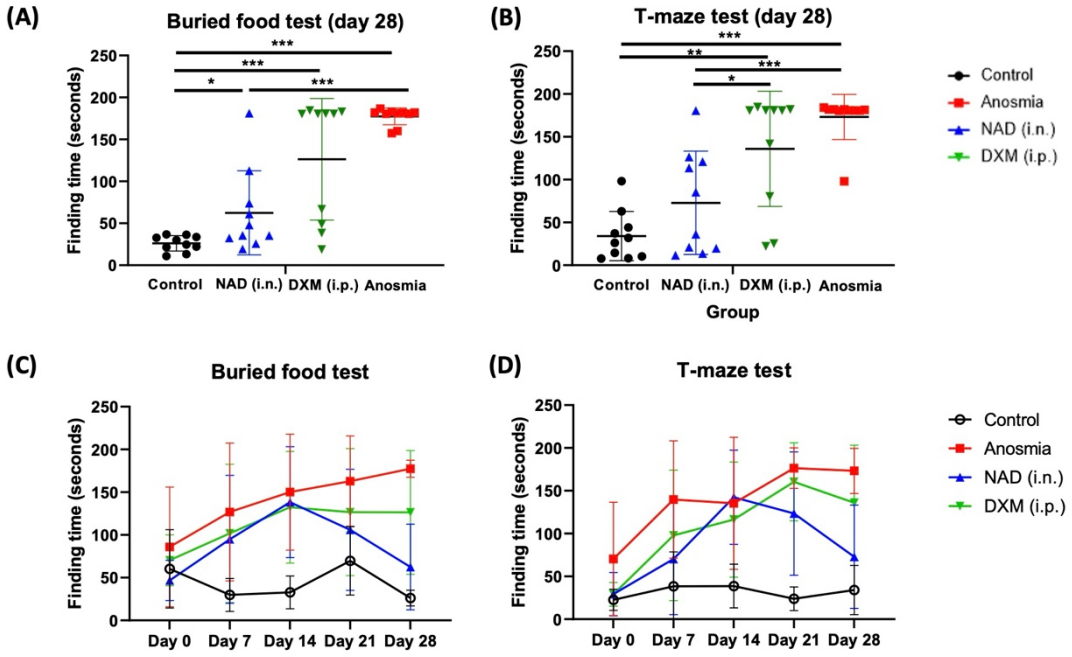

Figure 7. Histologic analyses of mouse olfactory epithelium (OE). (A) Hematoxylin and eosin (H&E) stained images of the olfactory mucosa in the nasal cavity. (B) Immunofluorescence (IF) stained images of the olfactory mucosa in the nasal cavity. (C) Thickness of the OE measured on H&E stained images. (D) Olfactory marker protein (OMP)-positive cells were evaluated on IF-stained images. (E) Mean fluorescence intensity (MFI) of acetylated β III-tubulin (Tuj1) was measured on IF-stained images. *P*-values were calculated using an independent sample *t*-test. * $P < 0.05$, ** $P < 0.01$, *** $P < 0.001$, n = 10 in each group.

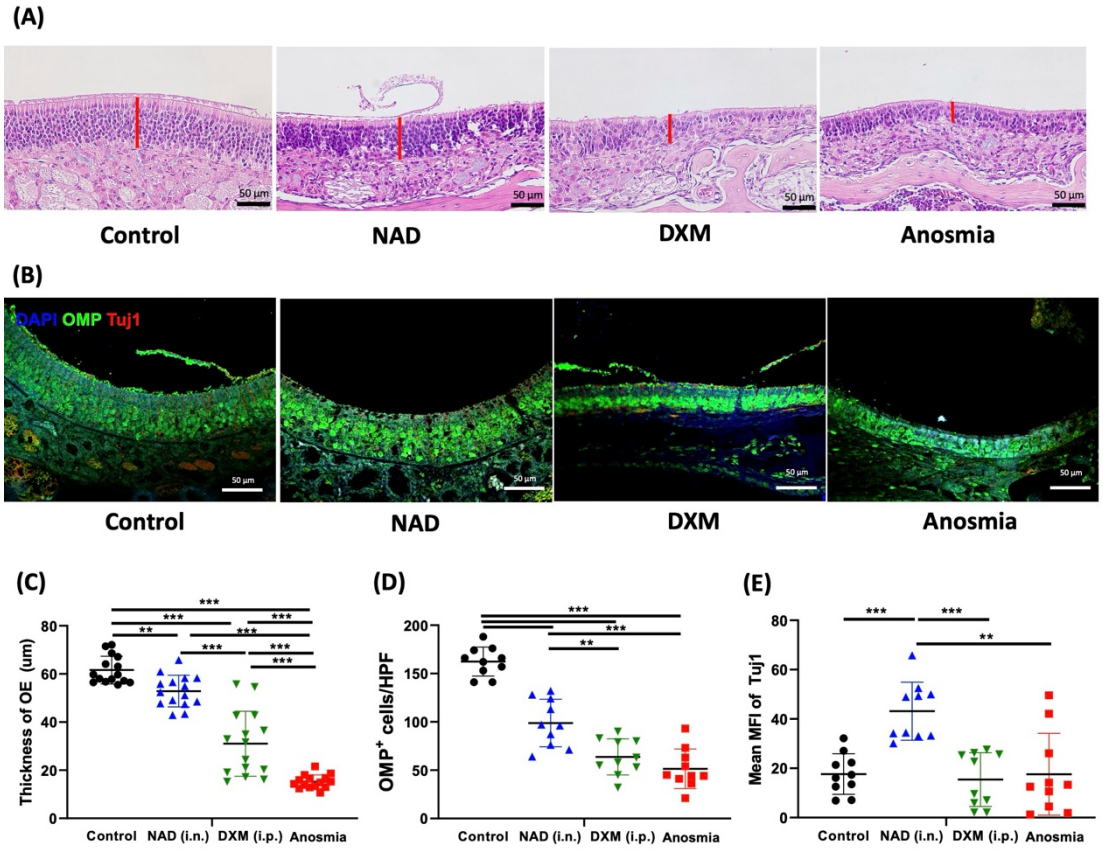

Comprehensive analysis of gene expression via RNA-seq analyses

RNA-seq was performed on olfactory turbinate tissues from the control, NAD, and anosmia groups to delineate their distinct and shared gene expression profiles (Figure 8A). Differences in the transcriptome profiles of olfactory turbinate tissues among these three groups were assessed. Principal component analysis (PCA), utilizing the expression data of all genes, distinctly classified the groups according to their respective conditions (Figure 8B). Within the olfactory turbinate, two unique gene expression patterns were identified, resulting in 201 differentially expressed genes (DEGs). Of these, 113 DEGs (Cluster T1) were upregulated in the control and NAD groups, whereas 88 (Cluster T2) were downregulated exclusively in the control group (Figure 8C). Gene Ontology (GO) analysis was used to decipher the molecular mechanisms and biological functions associated with genes in each identified cluster. The Go terms "modulation of chemical synaptic transmission", "regulation of nervous system process", and "response to steroid hormone" were associated with Cluster T1 (Figure 8D, left panel). In contrast, the GO terms "antigen processing and presentation", "innate immune response", and "inflammatory response" GO terms were associated with Cluster T2 (Figure 8D, right panel). Cellular deconvolution was subsequently applied using a validated public scRNA-seq dataset to identify candidate genes expressed in olfactory receptor neurons within the pool of identified genes.(28, 29) A total of 15,997 single cells from olfactory mucosa biopsies of healthy donors revealed diversity across 15 cell types, including neuronal populations, each distinguished by a unique profile of the top five DEGs (Figures 8E and 8F). Twenty-five genes implicated in the modulation of synaptic chemical transmission were upregulated after NAD stimulation (Figure 8G).

Furthermore, intersecting these genes with neuronal marker genes acquired using scRNA-seq analysis identified candidate genes (Figure 8H). Six candidate genes—*ABHD2, DLGAP2, FOXO3, HIPK2, KCNMA1,* and *PCDH17*—were found to be expressed in olfactory receptor neurons (Figure 8I). Additionally, the expression of these genes was significantly

upregulated in the NAD group compared with the anosmia group, with their expression levels being restored to levels similar to those observed in the control group (Figure 8J).

Figure 8. Comprehensive analysis of gene expression via RNA sequencing analyses. (A) Schematic representation of sample preparation from olfactory turbinate, followed by RNA extraction and computational analysis via RNA sequencing. (B) Principal component analysis (PCA) plots displaying sample clustering from olfactory turbinate in control, anosmia, and nicotinamide adenine dinucleotide (NAD)-treated mice. (C) Gene expression in mouse olfactory turbinate. Left: heatmap illustrating the expression levels of differentially expressed genes (DEGs) meeting specific criteria (false discovery rate [FDR] < 0.05; two-fold difference in expression level; average transcript per million [TPM] > 2). K-means clustering (k = 2) analysis of 201 DEGs across three groups, with values presented as z-score. Right: line graph depicting characteristic gene expression patterns for each cluster. (D) Gene ontology (GO) analysis was performed for Cluster T1 and T2 genes. (E) Uniform manifold approximation and projection (UMAP) visualization of single-cell RNA-seq data (GSE184117) for 15,997 single cells obtained from olfactory mucosa biopsies of healthy donors, categorizing cells into clusters based on gene expression profiles. (F) Heatmap showing top 5 differentially expressed genes across various cell types from olfactory mucosa biopsies of healthy donors, with gene expression intensity indicated by color gradient from low (green) to high (red). Values are z-scores. (G) Heatmap illustrating the expression patterns of genes related to modulation of chemical synaptic transmission within Cluster T1. (H) Venn diagram illustrating the overlap between genes related to modulation of chemical synaptic transmission and molecular markers of human olfactory neurons. (I) Violin plots depicting the distribution of normalized expression levels for selected genes related to the modulation of chemical synaptic transmission across different cell types, color-coded to match the cell types identified in Figure (D). (J) Graphs presenting TPM values for candidate genes. *P*-values were calculated using ordinary one-way ANOVA. * $P < 0.05$, ** $P < 0.01$, *** $P < 0.001$.

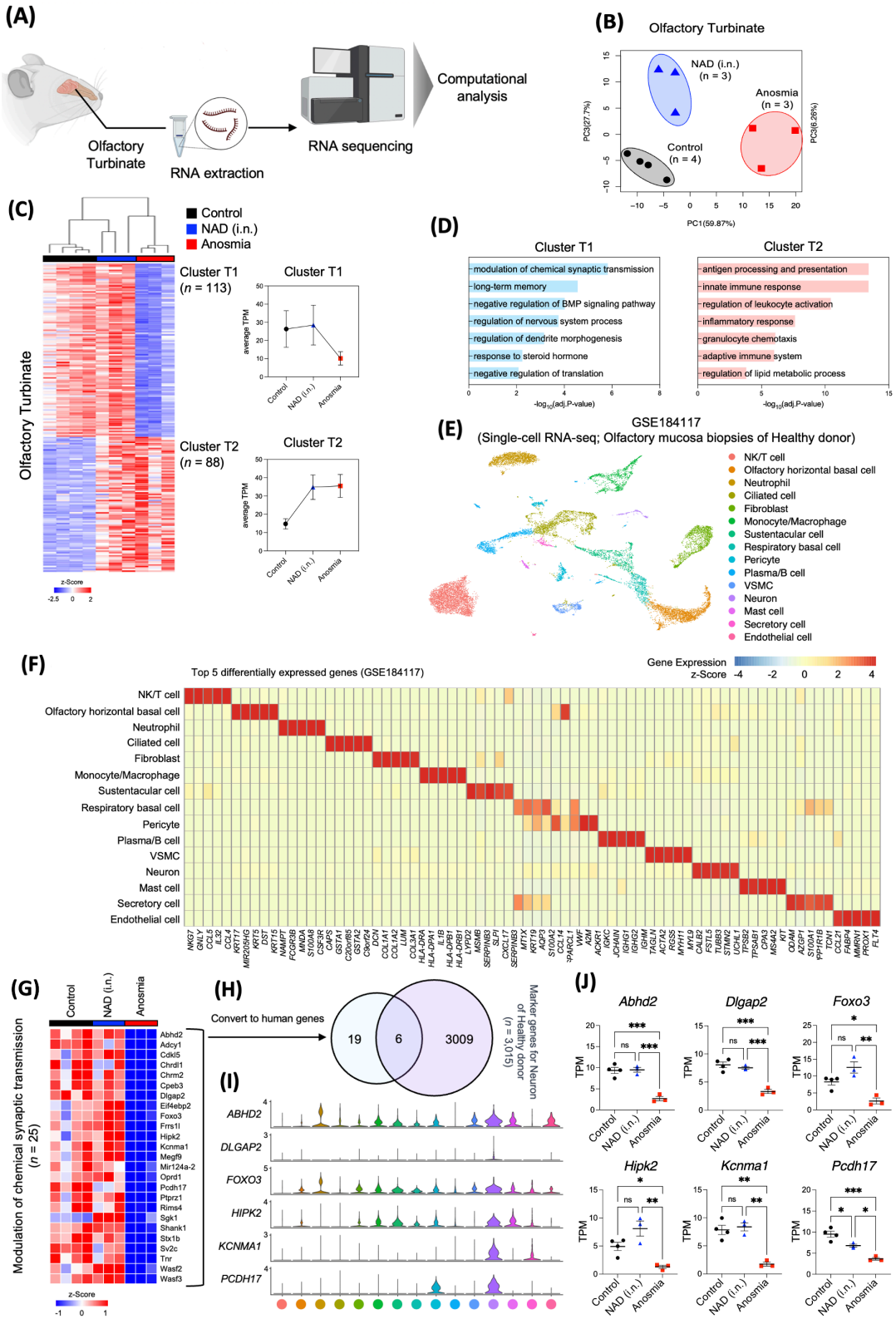

The genes identified from mouse olfactory RNA sequencing data were further validated using additional PCR analyses in hOSCs. From RNA-seq analyses, we found that six neuronal marker genes—*ABHD2, DLGAP2, FOXO3, HIPK2, KCNMA1*, and *PCDH17*—were upregulated in the NAD-treated group compared with the anosmia group. Subsequently, PCR analyses were conducted on four of these genes (Figure 9) in vitro. PCR analysis of the *KCNMA1* gene showed no significant differences between the NAD-treated group and the untreated group (data not shown), while the *ABHD2* gene was excluded from the analysis due to its predominant expression in oligodendrocytes in brain tissue and its undetermined function.(33) Among the remaining genes, *DLGAP2* (Figure 9A), *FOXO3* (Figure 9B), *HIPK2* (Figure 9C), and *PCDH17* (Figure 9D), the expression levels were significantly higher in the differentiated cell group compared with the undifferentiated hOSC group. Moreover, the NAD treatment group exhibited significantly higher levels of *FOXO3, HIPK2*, and *PCDH17* gene expression compared with the untreated group. Previous studies have associated these genes with cell survival, protection against oxidative stress, and nerve or cell regeneration.(34-37)

Figure 9. PCR analyses of four genes upregulated in the RNA sequencing analysis. PCR analysis confirmed the expression of each gene: *DLGAP2* (A), *FOXO3* (B), *HIPK2* (C), and *PCDH17* (D). The expression levels of these genes were analyzed under four distinct conditions: differentiation (-), differentiation (+) without nicotinamide adenine dinucleotide (NAD), and differentiation (+) with NAD. *P*-values were calculated using independent sample *t*-tests. * $P < 0.05$, ** $P < 0.01$, *** $P < 0.001$, n = 3 in each group.

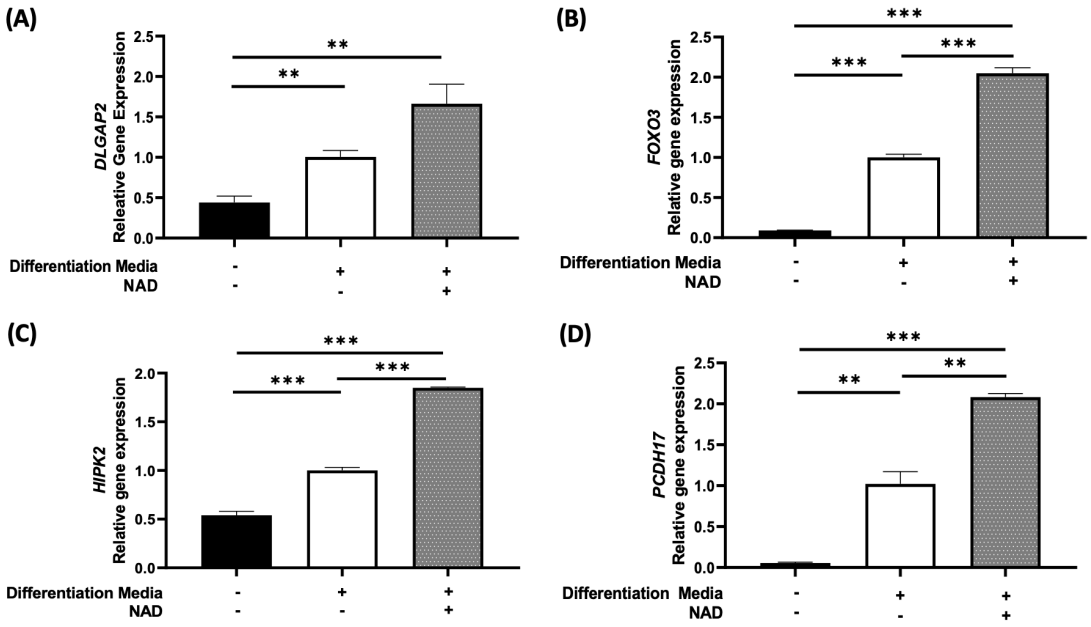

DISCUSSION

In this study, we explored the potential therapeutic role of NAD in addressing olfactory dysfunction using a mouse model of anosmia. Olfactory dysfunction is a prevalent condition that significantly impacts the quality of life and safety of individuals, potentially increasing mortality risk due to compromised detection of harmful odors and signals.(1-3, 11) Current treatments such as surgery, olfactory training, and steroid therapy, often lack guaranteed efficacy, posing challenges for effective management.(5, 9)

Initially, hOSCs were employed to assess the therapeutic efficacy of NAD in vitro. NAD facilitated the differentiation of hOSCs into OSNs, as evidenced by the IF staining of neuronal stem cell markers (SOX2, nestin) and OSN markers (OMP, acetylated β-III tubulin). PCR studies demonstrated that NAD increased the expression of markers associated with neuronal differentiation (*SOX2, NESTIN, NEUROD1, NEUROG1*, and *OMP*) in vitro. Additionally, Western blot analysis confirmed that NAD treatment elevated the levels of SOX2, nestin, and OMP proteins.

This study used a well-established mouse model of anosmia induced by intranasal $ZnSO_4$ administration. Experimental mice were categorized into four groups: control, anosmia, i.n. NAD treatment, and i.p. DXM injection. Behavioral tests, histological analyses, RNA sequencing, and in vitro experiments were conducted to evaluate the effects of NAD on olfactory function and its underlying mechanisms. Our results demonstrated that i.n. administration of NAD significantly improved olfactory function. This improvement was accompanied by enhanced neurogenesis and maturation of OSNs, as evidenced by behavioral tests and histological analyses. These findings are consistent with previous studies that highlighted the neuroprotective and neuroregenerative properties of NAD in various neurodegenerative disease models.(22, 23, 38) Of particular interest were the RNA sequencing results, which indicated upregulation of critical genes involved in neuronal development, chemical synaptic transmission, and olfactory sensory function in NAD-treated mice.

In vitro experiments provided mechanistic insights suggesting that NAD promotes the differentiation of human OSCs into mature OSNs. RNA-seq analysis of olfactory turbinate tissues identified two distinct gene expression patterns: upregulated genes (Cluster T1) in both the control and NAD-treated groups, and downregulated genes (Cluster T2) primarily in the control group (Figure 8C). Cluster T1 genes were predominantly associated with modulation of chemical synaptic transmission and long-term memory, while Cluster T2 genes were linked to inflammation and immune reactions. These findings indicate that NAD may enhance neurogenesis, synaptic plasticity, and the maturation of new OSNs, thereby facilitating functional recovery of olfaction. Interestingly, while Cluster T2 genes were related to immunological responses and inflammation, NAD treatment did not prevent these local immune responses in the olfactory mucosa.

In RNA-seq analysis, 25 genes involved in the modulation of synaptic chemical transmission were identified as upregulated after NAD stimulation. By intersecting these genes with human neuronal marker genes, six potential genes were significantly overexpressed in the NAD group compared with the anosmia group: *ABHD2, DLGAP2, FOXO3, HIPK2, KCNMA1,* and *PCDH17*. The expression of these genes increased to levels comparable to those in the control group. To further elucidate the mechanism, NAD-treated human OSCs were differentiated into OSNs, and PCR analysis was conducted for each candidate gene. The NAD-treated group showed elevated expression of *DLGAP2, FOXO3, HIPK2,* and *PCDH17* compared with the untreated group. All of these genes are expressed in the OSNs of OE.(28)

DLGAP2 encodes essential elements of postsynaptic scaffolding proteins crucial for synaptic morphogenesis and function.(39-41) It is implicated in regulating age-related neurodegeneration, cognitive decline, and Alzheimer's disease.(42) Based on the findings of this study, NAD administration likely mitigated olfactory neuronal degeneration by increasing *DLGAP2* expression.

Recent studies have highlighted the role of the *FOXO3* gene in regulating mammalian lifespan.(43, 44) Forkhead box transcription factors (FOXOs) such as FOXO3 are involved in

various physiological responses including cell cycle arrest, differentiation, resistance to oxidative stress, and apoptosis.(45) Research has demonstrated that FOXOs play a crucial role in enhancing the ability of adult hematopoietic and neural stem cells to regenerate by imparting resistance to oxidative stress.(46, 47) Additionally, NAD has been shown to promote neuronal survival under oxidative stress conditions through mechanisms involving protein kinase B and mitochondrial membrane potential, along with *FOXO3a*.(35) This observation that NAD treatment increased FOXO3 expression in this study suggests that NAD may prevent loss of olfactory function by enhancing the ability of OSNs to withstand oxidative stress.

HIPK2 encodes a serine/threonine kinase that is evolutionarily conserved.(48) It plays diverse roles in embryo development, stress response, and various pathological conditions including cancer and fibrosis. HIPK2 is abundantly expressed in both the central and peripheral nervous systems, and its genetic ablation in mice leads to neurological abnormalities. Moreover, *HIPK2* regulates the expression of genes involved in antioxidant production and response to reactive oxygen species.(49) In this study, NAD treatment was found to upregulate the expression of the *HIPK2* gene. Similar to the FOXO3 gene, it is hypothesized that HIPK2 expression promoted the survival of OSNs and facilitated the differentiation of OSCs into OSNs in environments with high oxidative stress.

Procadherins are members of the cadherin superfamily.(50) Previous research has indicated that procadherin genes, including *PCDH8, 10, 17, 18,* and *19,* regulate cell motility. For instance, depletion of *Pcdh19* during zebrafish embryonic neurulation leads to abnormal cell motility(51), while *Pcdh10* is essential for striatal axon formation in mice.(52) *PCDH17* mediates collective axon extension by recruiting actin regulator complexes to interaxonal contacts.(53) In this study, i.n. administration of NAD increased *PCDH17* expression, suggesting enhanced axonal extension during OSN regeneration.

In summary, NAD activates genes involved in synaptic transmission and neuronal survival under oxidative stress conditions. These genes include those that inhibit neuronal degeneration and promote OSN differentiation from OSNs. However, additional studies are

warranted to elucidate the specific mechanisms underlying the effects of NAD. Identifying these mechanisms could provide valuable insights into the pathological processes associated with anosmia.

Overall, this study shed light on a potential novel treatment approach for olfactory impairment and highlighted the need for further research to validate these results and explore the clinical applications of NAD in addressing olfactory dysfunction.

CONCLUSIONS

This study offers promising insights into the potential use of NAD as a therapeutic agent for treating olfactory dysfunction. We conducted comprehensive analyses of its effects on olfactory function, histology, gene expression, and in vitro differentiation using a mouse model and human OSCs. Further investigations and clinical trials are necessary to fully elucidate the clinical implications and safety profile of NAD-based therapies in patients with olfactory impairment.

REFERENCES

1. Hoffman HJ, Rawal S, Li CM, Duffy VB. New chemosensory component in the U.S. National Health and Nutrition Examination Survey (NHANES): first-year results for measured olfactory dysfunction. Rev Endocr Metab Disord. 2016;17(2):221-40.
2. Kern DW, Wroblewski KE, Schumm LP, Pinto JM, Chen RC, McClintock MK. Olfactory function in Wave 2 of the National Social Life, Health, and Aging Project. J Gerontol B Psychol Sci Soc Sci. 2014;69 Suppl 2(Suppl 2):S134-43.
3. Pinto JM, Wroblewski KE, Kern DW, Schumm LP, McClintock MK. Olfactory Dysfunction Predicts 5-Year Mortality in Older Adults. PLOS ONE. 2014;9(10):e107541.
4. Choi WR, Jeong HY, Kim JH. Reliability and validity of the Korean version of the Questionnaire of Olfactory Disorders. Int Forum Allergy Rhinol. 2018;8(12):1481-5.
5. Santos DV, Reiter ER, DiNardo LJ, Costanzo RM. Hazardous events associated with impaired olfactory function. Archives of otolaryngology--head & neck surgery. 2004;130(3):317-9.
6. Bonfils P, Faulcon P, Tavernier L, Bonfils NA, Malinvaud D. [Home accidents associated with anosmia]. Presse Med. 2008;37(5 Pt 1):742-5.
7. Miwa T, Furukawa M, Tsukatani T, Costanzo RM, DiNardo LJ, Reiter ER. Impact of olfactory impairment on quality of life and disability. Archives of otolaryngology--head & neck surgery. 2001;127(5):497-503.
8. Yoo SH, Kim H-W, Lee JH. Restoration of olfactory dysfunctions by nanomaterials and stem cells-based therapies: Current status and future perspectives. Journal of Tissue Engineering. 2022;13:20417314221083414.
9. Ku JY, Lee MK, Choi WR, Lee JH, Kim JH. Effect of olfactory bulb atrophy on the success of olfactory training. European Archives of Oto-Rhino-Laryngology. 2022;279(3):1383-9.
10. Chung MS, Choi WR, Jeong HY, Lee JH, Kim JH. MR Imaging-Based Evaluations of Olfactory Bulb Atrophy in Patients with Olfactory Dysfunction. AJNR Am J Neuroradiol. 2018;39(3):532-7.
11. Whitcroft KL, Altundag A, Balungwe P, Boscolo-Rizzo P, Douglas R, Enecilla MLB, et al. Position paper on olfactory dysfunction: 2023. Rhinology. 2023;61(33):1-108.
12. Ying W. NAD+/NADH and NADP+/NADPH in cellular functions and cell death: regulation and biological consequences. Antioxid Redox Signal. 2008;10(2):179-206.
13. Liu L, Su X, Quinn WJ, 3rd, Hui S, Krukenberg K, Frederick DW, et al. Quantitative Analysis of NAD Synthesis-Breakdown Fluxes. Cell Metab. 2018;27(5):1067-80.e5.
14. Navarro MN, Gómez de Las Heras MM, Mittelbrunn M. Nicotinamide adenine dinucleotide metabolism in the immune response, autoimmunity and inflammageing. Br J Pharmacol. 2022;179(9):1839-56.
15. Essuman K, Summers DW, Sasaki Y, Mao X, DiAntonio A, Milbrandt J. The SARM1 Toll/Interleukin-1 Receptor Domain Possesses Intrinsic NAD(+) Cleavage Activity that Promotes Pathological Axonal Degeneration. Neuron. 2017;93(6):1334-43.e5.
16. Nikiforov A, Kulikova V, Ziegler M. The human NAD metabolome: Functions, metabolism

and compartmentalization. Crit Rev Biochem Mol Biol. 2015;50(4):284-97.
17. Ziegler M, Oei SL. A cellular survival switch: poly(ADP-ribosyl)ation stimulates DNA repair and silences transcription. Bioessays. 2001;23(6):543-8.
18. Luo X, Kraus WL. On PAR with PARP: cellular stress signaling through poly(ADP-ribose) and PARP-1. Genes Dev. 2012;26(5):417-32.
19. Cantó C, Menzies KJ, Auwerx J. NAD(+) Metabolism and the Control of Energy Homeostasis: A Balancing Act between Mitochondria and the Nucleus. Cell Metab. 2015;22(1):31-53.
20. Demarest TG, Babbar M, Okur MN, Dan X, Croteau DL, Fakouri NB, et al. NAD+ metabolism in aging and cancer. Annual Review of Cancer Biology. 2019;3:105-30.
21. Lautrup S, Sinclair DA, Mattson MP, Fang EF. NAD(+) in Brain Aging and Neurodegenerative Disorders. Cell Metab. 2019;30(4):630-55.
22. Lautrup S, Sinclair DA, Mattson MP, Fang EF. NAD+ in brain aging and neurodegenerative disorders. Cell metabolism. 2019;30(4):630-55.
23. Ying W, Wei G, Wang D, Wang Q, Tang X, Shi J, et al. Intranasal administration with NAD+ profoundly decreases brain injury in a rat model of transient focal ischemia. Front Biosci. 2007;12:2728-34.
24. Girard SD, Devéze A, Nivet E, Gepner B, Roman FS, Féron F. Isolating nasal olfactory stem cells from rodents or humans. J Vis Exp. 2011(54).
25. Dobin A, Davis CA, Schlesinger F, Drenkow J, Zaleski C, Jha S, et al. STAR: ultrafast universal RNA-seq aligner. Bioinformatics. 2013;29(1):15-21.
26. Heinz S, Benner C, Spann N, Bertolino E, Lin YC, Laslo P, et al. Simple combinations of lineage-determining transcription factors prime cis-regulatory elements required for macrophage and B cell identities. Mol Cell. 2010;38(4):576-89.
27. Love MI, Huber W, Anders S. Moderated estimation of fold change and dispersion for RNA-seq data with DESeq2. Genome Biology. 2014;15(12):550.
28. Oliva AD, Gupta R, Issa K, Abi Hachem R, Jang DW, Wellford SA, et al. Aging-related olfactory loss is associated with olfactory stem cell transcriptional alterations in humans. J Clin Invest. 2022;132(4).
29. Tepe B, Hill MC, Pekarek BT, Hunt PJ, Martin TJ, Martin JF, Arenkiel BR. Single-Cell RNA-Seq of Mouse Olfactory Bulb Reveals Cellular Heterogeneity and Activity-Dependent Molecular Census of Adult-Born Neurons. Cell Rep. 2018;25(10):2689-703.e3.
30. Ellis P, Fagan BM, Magness ST, Hutton S, Taranova O, Hayashi S, et al. SOX2, a persistent marker for multipotential neural stem cells derived from embryonic stem cells, the embryo or the adult. Dev Neurosci. 2004;26(2-4):148-65.
31. Borgmann-Winter K, Willard SL, Sinclair D, Mirza N, Turetsky B, Berretta S, Hahn CG. Translational potential of olfactory mucosa for the study of neuropsychiatric illness. Translational Psychiatry. 2015;5(3):e527-e.
32. Bernal A, Arranz L. Nestin-expressing progenitor cells: function, identity and therapeutic implications. Cellular and Molecular Life Sciences. 2018;75(12):2177-95.

33. Fazio D, Criscuolo E, Maccarrone M. Radiometric Assay of ABHD2 Activity. Methods Mol Biol. 2023;2576:299-305.
34. Jiang F, Zhu Y, Chen Y, Tang X, Liu L, Chen G, et al. Progesterone activates the cyclic AMP-protein kinase A signalling pathway by upregulating ABHD2 in fertile men. Journal of International Medical Research. 2021;49(3):0300060521999527.
35. Chong ZZ, Lin SH, Maiese K. The NAD+ precursor nicotinamide governs neuronal survival during oxidative stress through protein kinase B coupled to FOXO3a and mitochondrial membrane potential. J Cereb Blood Flow Metab. 2004;24(7):728-43.
36. Dang X, Zhang R, Peng Z, Qin Y, Sun J, Niu Z, Pei H. HIPK2 overexpression relieves hypoxia/reoxygenation-induced apoptosis and oxidative damage of cardiomyocytes through enhancement of the Nrf2/ARE signaling pathway. Chem Biol Interact. 2020;316:108922.
37. Hoshina N, Tanimura A, Yamasaki M, Inoue T, Fukabori R, Kuroda T, et al. Protocadherin 17 regulates presynaptic assembly in topographic corticobasal Ganglia circuits. Neuron. 2013;78(5):839-54.
38. Hou Y, Lautrup S, Cordonnier S, Wang Y, Croteau DL, Zavala E, et al. NAD(+) supplementation normalizes key Alzheimer's features and DNA damage responses in a new AD mouse model with introduced DNA repair deficiency. Proc Natl Acad Sci U S A. 2018;115(8):E1876-e85.
39. Takeuchi M, Hata Y, Hirao K, Toyoda A, Irie M, Takai Y. SAPAPs. A family of PSD-95/SAP90-associated proteins localized at postsynaptic density. J Biol Chem. 1997;272(18):11943-51.
40. Kim E, Naisbitt S, Hsueh YP, Rao A, Rothschild A, Craig AM, Sheng M. GKAP, a novel synaptic protein that interacts with the guanylate kinase-like domain of the PSD-95/SAP90 family of channel clustering molecules. J Cell Biol. 1997;136(3):669-78.
41. Welch JM, Wang D, Feng G. Differential mRNA expression and protein localization of the SAP90/PSD-95-associated proteins (SAPAPs) in the nervous system of the mouse. J Comp Neurol. 2004;472(1):24-39.
42. Ouellette AR, Neuner SM, Dumitrescu L, Anderson LC, Gatti DM, Mahoney ER, et al. Cross-Species Analyses Identify Dlgap2 as a Regulator of Age-Related Cognitive Decline and Alzheimer's Dementia. Cell Rep. 2020;32(9):108091.
43. Flachsbart F, Caliebe A, Kleindorp R, Blanché H, von Eller-Eberstein H, Nikolaus S, et al. Association of FOXO3A variation with human longevity confirmed in German centenarians. Proc Natl Acad Sci U S A. 2009;106(8):2700-5.
44. Willcox BJ, Donlon TA, He Q, Chen R, Grove JS, Yano K, et al. FOXO3A genotype is strongly associated with human longevity. Proc Natl Acad Sci U S A. 2008;105(37):13987-92.
45. Salih DA, Brunet A. FoxO transcription factors in the maintenance of cellular homeostasis during aging. Curr Opin Cell Biol. 2008;20(2):126-36.
46. Miyamoto K, Araki KY, Naka K, Arai F, Takubo K, Yamazaki S, et al. Foxo3a is essential for maintenance of the hematopoietic stem cell pool. Cell Stem Cell. 2007;1(1):101-12.
47. Tothova Z, Kollipara R, Huntly BJ, Lee BH, Castrillon DH, Cullen DE, et al. FoxOs are critical mediators of hematopoietic stem cell resistance to physiologic oxidative stress. Cell.

2007;128(2):325-39.

48. Kim YH, Choi CY, Lee S-J, Conti MA, Kim Y. Homeodomain-interacting Protein Kinases, a Novel Family of Co-repressors for Homeodomain Transcription Factors *. Journal of Biological Chemistry. 1998;273(40):25875-9.

49. de la Vega L, Grishina I, Moreno R, Krüger M, Braun T, Schmitz ML. A Redox-Regulated SUMO/Acetylation Switch of HIPK2 Controls the Survival Threshold to Oxidative Stress. Molecular Cell. 2012;46(4):472-83.

50. Hulpiau P, van Roy F. Molecular evolution of the cadherin superfamily. Int J Biochem Cell Biol. 2009;41(2):349-69.

51. Biswas S, Emond MR, Jontes JD. Protocadherin-19 and N-cadherin interact to control cell movements during anterior neurulation. J Cell Biol. 2010;191(5):1029-41.

52. Uemura M, Nakao S, Suzuki ST, Takeichi M, Hirano S. OL-Protocadherin is essential for growth of striatal axons and thalamocortical projections. Nat Neurosci. 2007;10(9):1151-9.

53. Hayashi S, Inoue Y, Kiyonari H, Abe T, Misaki K, Moriguchi H, et al. Protocadherin-17 mediates collective axon extension by recruiting actin regulator complexes to interaxonal contacts. Dev Cell. 2014;30(6):673-87.

국문 요약

후각장애는 냄새를 잘 맡지 못하거나 아예 후각을 상실하는 상태로 후각뿐만 아니라 미각에도 영향을 끼쳐 환자의 삶의 질을 현저히 떨어뜨리지만 현재까지 확립된 치료법은 없는 현실이다. 본 연구에서는 후각 장애 회복을 위해 비강 내 투여된 니코틴아미드 아데닌 디뉴클레오티드(NAD)의 효능을 평가하였다.

본 연구는 음성 대조군, 양성 대조군, 비강내 NAD 투여군, 복강내 스테로이드 투여군의 4개의 마우스 모델 그룹을 활용하여 동물 실험을 시행하였다 (각 군당 10마리). 음성 대조군은 정상 후각군으로 PBS만을 투여하였으며, 나머지 세 군은 $ZnSO_4$ 의 비강내 투여를 통해 후각 상실 마우스 모델을 제작하였다. 양성 대조군은 치료물질 대신 PBS 비강 내 투여를 시행하였다. 총 4주간 모델 제작 및 약물 투여를 시행하였으며 매주 후각 기능 행동 평가를 시행하였고, 이후에는 마우스의 후각 상피의 조직 염색[hematoxylin and eosin(H&E) 및 면역형광염색]을 시행하여 후각 상피의 조직학적 회복 정도를 평가하였다. 추가적인 분석을 RNA 시퀀싱 분석을 통해 시행하였고, 인간 후각 줄기 세포에 NAD를 처리하여 실제로 후각 신경 세포로의 분화가 촉진되는지 세포실험을 통해 확인하였다.

동물 행동 실험 결과, 비강내 NAD 투여군에서 후각 기능이 가장 잘 보존된 것으로 확인하였다. 또한 조직학적 분석 결과 NAD 투여군의 후각 상피가 가장 잘 보존 된 것으로 확인하였다. 후각 상피의 두께 및 후각 신경 세포의 개수 모두 NAD 군에서 통계적으로 유의미하게 더 높았다.

더불어 RNA 시퀀싱 분석을 통해 이와 관련된 6개의 후보 유전자를 확인하였다. 이들 유전자는 양성 대조군(후각상실 마우스)과 후각상실증 모델과 비교하여

NAD 군 마우스에서 발현이 증가됨을 확인하였고, 이들의 발현 수준은 음성 대조 마우스 모델에서 관찰된 것과 유사한 것을 확인하였다. 세포 실험에서는 인간 후각 줄기세포의 NAD를 처리하였을 때 후각 신경 세포로의 분화가 촉진됨을 확인하였다.

본 연구는 후각상실 마우스 모델 실험을 통해 비강 내 NAD 투여의 치료 효능을 확인하였고 인간 후각 상피 줄기세포에서 NAD의 투여가 후각 신경 세포로의 분화를 촉진시킴을 확인하였다. 이러한 결과를 종합하여 저자는 NAD의 후각 상실 치료제로서의 개발 가능성을 제시하는 바이다.